Applied Energy 365 (2024) 123275

Contents lists available at ScienceDirect

Applied Energy

journal homepage: www.elsevier.com/locate/apenergy

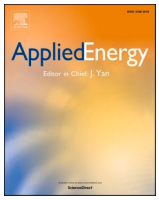

A CCP-based distributed cooperative operation strategy for multi-agent energy systems integrated with wind, solar, and buildings

Bing Ding [a,b], Zening Li [a,b,*], Zhengmao Li [d], Yixun Xue [a,b], Xinyue Chang [a,b], Jia Su [a,b], Xiaolong Jin [e], Hongbin Sun [a,b,c,*]

[a] College of Electrical and Power Engineering, Taiyuan University of Technology, Taiyuan 030024, China
[b] Key Laboratory of Cleaner Intelligent Control on Coal & Electricity, Ministry of Education, Taiyuan University of Technology, Taiyuan 030024, China
[c] Department of Electrical Engineering, Tsinghua University, Beijing 100084, China
[d] School of Electrical Engineering, Aalto University, 02150 Espoo, Finland
[e] Key Laboratory of Smart Grid of Ministry of Education, Tianjin University, Tianjin 300072, China

HIGHLIGHTS

- A distributed cooperative operation strategy for multi-agent energy systems integrated with wind, solar, and buildings is proposed.
- Bidirectional interactions between wind/solar power plant and buildings are realized by the Nash bargaining-based incentive cooperative mechanism.
- Indoor temperature comfort in buildings is ensured under diverse uncertainties by exploring the building flexibility through chance-constrained programming.
- Power trading results and the economy of the energy system and the participating agents are analyzed.

ARTICLE INFO

Keywords:
Alternating direction method of multipliers
Buildings
Chance-constrained programming
Multi-agent energy systems
Nash bargaining

ABSTRACT

To explore the bidirectional interaction between renewable energy and buildings in multi-agent energy systems, this paper proposes a distributed cooperative operation strategy for multi-agent energy systems integrated with wind, solar, and buildings based on chance-constrained programming (CCP). First, the multi-agent energy system integrated with wind, solar, and buildings is comprehensively modeled with detailed electric and thermal characteristics for flexibility enhancement. Then for maximizing the profits of the cooperative energy system and each engaged agent, a Nash bargaining model is presented and is divided into two subproblems: the coalition income and the power payment. To preserve the privacy of agents, the adaptive alternating direction method of multipliers (ADMM) is exploited to solve both subproblems. Meanwhile, the CCP method is applied to address diverse uncertainties from wind and solar power generation as well as outdoor temperature. Finally, the effectiveness of the proposed strategy is validated. The simulation results show that, besides the privacy of information among all agents being well preserved, our strategy enhances the profits not only for the energy system but also for all engaged agents.

1. Introduction

International Energy Agency (IEA) forecasts that by 2030, global natural gas and oil demand will be around 4500 billion cubic meters and 104 million barrels per day [1]. With the skyrocketing energy demands, the world now is under the highest pressure ever and trying to process the energy transition from the perspective of energy generation and consumption [2].

From the energy generation perspective, the key is exploring renewable energy sources, such as wind and solar power, to replace fossil fuels [3]. By the end of 2022, global renewable generation capacity (GC) amounted to around 3372 GW, growing the stock of renewable power by 9.6% [4]. With policy support, many renewable energy projects are launched worldwide. In Gujarat, India, the world's largest renewable energy park of 30 GW capacity solar-wind hybrid project is under installation [5]. As electricity from renewable energy continues increasing rapidly, efforts are made by countries to encourage

* Corresponding authors at: College of Electrical and Power Engineering, Taiyuan University of Technology, Taiyuan 030024, China.
E-mail addresses: lizening@tyut.edu.cn (Z. Li), zhengmao.li@aalto.fi (Z. Li), xueyixun@tyut.edu.cn (Y. Xue), sujia@tyut.edu.cn (J. Su), xljin@tju.edu.cn (X. Jin), shb@tsinghua.edu.cn (H. Sun).

https://doi.org/10.1016/j.apenergy.2024.123275
Received 18 January 2024; Received in revised form 5 April 2024; Accepted 17 April 2024
Available online 25 April 2024

Nomenclature

Abbreviations

AC	Air conditioner
ADMM	Alternating direction method of multipliers
AM-GM	Arithmetic mean-geometric mean
CCP	Chance-constrained programming
CIS	Coalition income subproblem
DPP	Direct power purchase
PG	Power grid
PPS	Power payment subproblem
TDM	Thermal dynamic model
SPP	Solar power plant
WPP	Wind power plant

Indices and sets

i, j	Index of nodes
n	Index of rooms
t	Index of time periods
N_{room}	Number of rooms in a building
$N_{\text{room},n}$	Set of adjacent room nodes of the room n
$N_{\text{wall},n}$	Set of adjacent wall nodes of the room n
$N_{\text{win},n}$	Set of wall nodes with window of the room n

Parameters and constants

$A_{\text{wall},ij}/A_{\text{win},ij}$	Area of the wall/window between ith and jth node (m^2)
$C_{\text{room},k}/C_{\text{wall},ij}$	Heat capacity of the kth room and the wall between ith and jth node (J/K)
$I0$ w/$I0$ s/$C0$ b	Negotiation rupture points for bargaining of WPP/SPP/the buildings ($)
E_{EER}	Energy efficiency ratio
Et,max out	Maximum prediction error percentage of the outdoor temperature at the time t
Et,max w/Et,max s	Maximum prediction error percentage of wind/solar power generation at the time t
Pmax AC	Maximum operating power of ACs (kW)
pt bg	Day-ahead market prices at the time t ($/kWh)
Pt nm	Power of normal loads at the time t (kWh)
Pt w/Pt s	Predictive wind/solar power generation at the time t (kWh)
$p_{\text{w2g}}/p_{\text{s2g}}$	Wind/solar power feed-in tariff ($/kWh)
Qt rad,ij/Qt rad,n	Radiant heat flow density on the wall/window (W/m^2)
Qt int,n	Internal heat gain (W)
r_{ij}/π_{ij}	Sunlit wall/window identifier
R_t	Random number in the range of [−1,1] representing the prediction uncertainty
$R_{\text{wall},ij}/R_{\text{win},ij}$	Thermal resistance of the wall/window
T	Total operation horizon
Tt out	Predictive outdoor temperature (°C)
Tmin,lim room/Tmax,lim room	Limited minimum/maximum indoor temperature (°C)
Tmin room/Tmax room	Minimum/maximum comfort indoor temperature (°C)
v_{ij}	Absorption coefficient of walls
w_{ij}	Window transmittance coefficient
α_s, β_s	Coefficients of the wheeling cost of SPP
α_w, β_w	Coefficients of the wheeling cost of WPP
η	Probability that the indoor temperature can be completely constrained in the comfort range
$\kappa_{\text{nm}}/\kappa_{\text{AC}}$	Coefficient of the maintenance costs of normal loads/ACs ($/kWh)
κ_w/κ_s	Coefficient of the maintenance cost of WPP/SPP ($/kWh)
λt w, λt s, γt w, γt s	Lagrange multipliers
ρ_w, ρ_s, ψ_w, ψ_s	Penalty parameters
Δt	Time interval

Variables

C_b	Cost of the buildings ($)
C_{bg}	Electricity cost of the buildings from PG ($)
C_{bm}	Maintenance cost of the buildings ($)
$C_{\text{sg}}/C_{\text{sm}}$	Wheeling/maintenance cost of SPP ($)
$C_{\text{wg}}/C_{\text{wm}}$	Wheeling/maintenance cost of WPP ($)
I_w/I_s	Income of WPP/SPP ($)
$I_{\text{s2b}}/I_{\text{s2g}}$	Income of SPP by selling electricity to the buildings/PG ($)
$I_{\text{w2b}}/I_{\text{w2g}}$	Income of WPP by selling electricity to the buildings/PG ($)
Pt bg	Electricity amount purchased from PG by the buildings (kWh)
Pt AC	Electricity consumption of ACs at the time t (kWh)
Pt AC,n	Power of the AC in the room n (kW)
Pt' w/Pt' s	Real wind/solar power generation at the time t (kWh)
pt w2b/pt s2b	Trading prices between WPP/SPP and the buildings at the time t ($/kWh)
Pt s2b/Pt s2g	Electricity amount that SPP trades with the buildings/PG at the time t (kWh)
Pt w2b/Pt w2g	Electricity amount that WPP trades with the buildings/PG at the time t (kWh)
Tt j	Temperature of jth node at the time t (°C)
Tt room,n	Indoor temperature at the time t (°C)
γt n	Boolean variable for the room n at the time t

renewable energy consumption. For instance, in the U.S., certain states have restructured their electricity industry to improve market competition, allowing consumers to choose not only how electricity is generated, but also who generates it [6].

From the energy consumption perspective, the building sector, which accounts for approximately 30% of global energy consumption, plays an important role in the energy transition [7]. With urbanization and improvements in living standards, the ever-increasing demand for indoor temperature comfort has led to the widespread use of air conditioners (ACs). It is forecasted that the adoption rate of ACs will jump from 37% of the global population to nearly 45% in 2030 [8]. Maintaining comfortable indoor temperature has become one of the leading drivers of rising electricity demand in buildings. It becomes crucial to strike a balance between energy conservation and indoor temperature comfort. Incorporating design strategies for flexibly adjusting indoor temperature into the thermal inertia of the building envelope [9] and guiding end-users in using electricity rationally [10] can contribute to improving energy efficiency and reducing energy consumption.

Combining energy-efficient building design with renewable energy can create a powerful synergy. Several countries have strengthened building regulations. In 2022, an energy conservation code introduced by India highlighted that buildings may be required to meet a proportion of their energy needs from renewable energy sources [11]. Although progress and policies regarding the development of renewable energy and energy-efficient buildings continue to expand, gaps remain. The lack of suitable mechanisms that can stimulate consumers to trade with renewable energy generation is a great challenge for accommodating renewable energy into buildings. Nash bargaining, which is a cooperative game in game theory, has been widely applied to cooperative optimization problems of distributed energy systems for obtaining

equitable distribution schemes [12]. A fair cost-sharing method based on Nash bargaining to incentivize cooperative planning, such that all microgrids will benefit from cooperative planning, is shown in Ref. [13]. Nash bargaining is adopted to design a benefit allocation mechanism for microgrids in Ref. [14]. The research in Ref. [15] proposes a Nash bargaining framework to describe how the carbon-capture-utilization-and-storage system works with distributed energy resources cooperatively. Ref. [16] uses Nash bargaining to characterize the trading behavior of stakeholders and obtain a fair benefit distribution scheme for multi-energy microgrids. A multi-agent electricity-heat-hydrogen peer-to-peer trading optimization model is solved based on Nash bargaining in Ref. [17]. Nash bargaining is used to redistribute benefits between shared energy storage systems and multi-microgrids to maintain long-term cooperation in Ref. [18]. The above research provides great opinions on building an incentive trading mechanism for multi-agent energy systems, but the buildings, as a type of large-scale natural and flexible resources on the load side, are rarely considered independent agents to participate directly in electricity trading.

While the trading mechanism is being explored, information sharing becomes an issue that needs to be considered. The model of a grid-connected hybrid power system depicted in Ref. [19] assumes that all the involved information is open. The game theory-based trading method for microgrid parks proposed in Ref. [20] utilizes a central controller to collect and distribute information. Though centralized methods are efficient for transactions, considering the agents' reluctance to share data, it is necessary and crucial to formulate a proper privacy protection mechanism [21]. Many studies have adopted distributed methods to protect privacy like the alternating direction method of multipliers (ADMM) approach [22]. Since ADMM can divide a centralized problem into subproblems that can be solved by agents independently and locally, while only intermediate parameters need to be shared, the ADMM method can be effective in ensuring the privacy of agents [23]. Ref. [24] uses the ADMM method as a privacy-preserving solution to the formulated security-constrained peer-to-peer transactive energy trading model. Ref. [25] proposes an optimal operation strategy considering negotiation pricing for tradable green certificates and uses the ADMM method for distributed solutions to ensure the information privacy of the transaction agent. Ref. [26] provides a distributed solution method based on ADMM to avoid the privacy information leakage of virtual energy stations and integrated energy systems. In Ref. [27], the ADMM method is applied to solve the data privacy issue for a comprehensive scheduling framework. Ref. [28] shows that the increased privacy follows from the distribution of information based on ADMM. Though the ADMM method is employed in areas like energy systems, operating schedules, and frequency reserve, few studies have investigated its performance in the operation of the multi-agent energy system integrated with wind, solar, and buildings.

Another big challenge lies in the handling of diverse uncertainties from wind and solar power generation as well as outdoor temperature, which will influence the operation of the multi-agent energy system [29]. To accurately describe the uncertainties mentioned above, the chance-constrained programming (CCP) method could be employed. This method can relax the original hard constraints based on the practical needs, i.e., the probability of meeting constraints is set to be not lower than a certain confidence level. The CCP method can be applied to deal with the randomness of frequency regulation requirements for ensuring battery energy storage systems profit from the energy arbitrage strategy in Ref. [30]. In Ref. [31], all uncertain parameters such as the load demand, nominal voltages, and facility failure rates are handled by utilizing the CCP approach. Ref. [32] proposes the CCP method to model the impact of load uncertainties on energy reserve constraints. Ref. [33] provides a method based on CCP to account for multiple uncertainties from energy/traffic demand and renewable generations. In Ref. [34], a method based on CCP is applied to deal with the uncertainty from both renewable generations and the flexibility of distributed energy resources. As changes in confidence levels in the CCP method can adjust the conservatism of optimization models, it can be further used to explore the economy of multi-agent energy systems under diverse uncertainties [35].

With the above, a CCP-based optimal distributed cooperative operation strategy is proposed for multi-agent energy systems integrated with wind, solar, and buildings. The main contributions of this study are summed up in the following aspects:

1) An incentive mechanism through Nash bargaining is proposed for the multi-agent energy system integrated with wind, solar, and buildings. Bidirectional interactions between the wind power plant (WPP) and the buildings, as well as the solar power plant (SPP) and the buildings, are realized. Agents are motivated to cooperate for profit improvement.
2) A CCP-based operation strategy is proposed to cope with the uncertainties of the outdoor environment and to explore the building flexibility considering the thermal inertia of the building envelope, while the comfort of all consumers can be ensured.
3) The adaptive ADMM is exploited to solve the Nash bargaining model in a distributed way so that the privacy of WPP, SPP, and the buildings can be effectively protected with the optimal operation strategy obtained.

The paper is organized as follows: Section II gives the problem description. Section III gives the system models. Section IV introduces the solving strategies including the conversion of deterministic constraints and Nash bargaining model. Section V gives case studies. Section VI gives the conclusions of the research.

2. Problem description

In this section, the framework of the multi-agent energy system integrated with wind, solar, and buildings is presented in Fig. 1.

The energy system consists of three agents, namely WPP, SPP, and the buildings. In the conventional trading mode, three agents will operate independently, i.e., the buildings purchase electricity from the power grid (PG), and WPP and SPP generate and sell electricity to PG for profits. Although this mode promotes the development and consumption of wind and solar power, it results in inefficient operation and management of each agent because there is no communication among agents regarding information such as demand, trading amount, and price. This leads to disordered competition that adversely impacts the operation of WPP, SPP, and the buildings. Thus, to enhance the competitiveness of WPP and SPP in the electricity market and to improve the profits of WPP, SPP, and the buildings, finding an optimal cooperative operation framework is necessary.

With the diversified electricity market entities, direct power purchase (DPP) is one of the main enriched power trading methods [36]. DPP is a transaction form in which enterprises or individuals with a certain power consumption scale purchase electricity from generation units. Based on DPP, this study proposes a framework where WPP and SPP sign agreements with the buildings to sell electricity directly. In the transaction, to increase profits, WPP and SPP bargain with the buildings over the trading electricity amount and prices based on the information of supply and demand till the agreement is reached. Meanwhile, to supply electricity, WPP and SPP need to use the grid of PG, so they sign the agreement with PG for the connection and use of the system and pay the wheeling cost to PG [37]. Besides, WPP and SPP sell the surplus electricity to PG to improve the profits. The buildings can select to purchase electricity from PG, WPP, and SPP to reduce the operation cost. Through this framework, three agents are motivated to cooperate, as well as wind and solar power can be accommodated adequately, contributing to sustainable energy development.

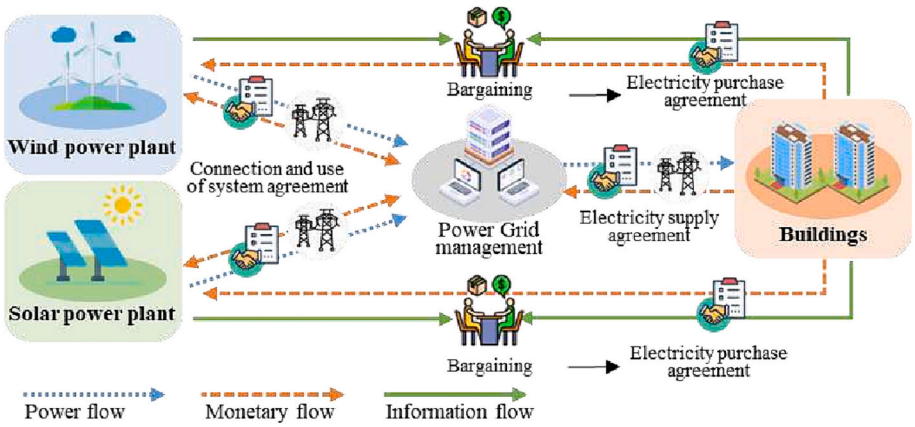

Fig. 1. The framework of the multi-agent energy system.

3. System models

3.1. Wind power plant

3.1.1. The trading model

In this study, WPP sells electricity to PG at the feed-in tariff and to the buildings at the negotiated prices. Thus, its income can be formulated as follows [12]:

$$I_{w2g} = \sum_{t=1}^{T} p_{w2g} P_{w2g}^{t} \tag{1}$$

$$I_{w2b} = \sum_{t=1}^{T} p_{w2b}^{t} P_{w2b}^{t} \tag{2}$$

The costs of WPP include the maintenance cost C_{wm} and the wheeling cost C_{wg}, which can be formulated as:

$$C_{wm} = \sum_{t=1}^{T} \kappa_w P_w^t \tag{3}$$

$$C_{wg} = \sum_{t=1}^{T} \left(\alpha_w {P_{w2b}^{t}}^2 + \beta_w P_{w2b}^{t} \right) \tag{4}$$

The trading electricity amount should satisfy the following:

$$0 \le P_{w2g}^{t} \le P_w^t \tag{5}$$

$$0 \le P_{w2b}^{t} \le P_w^t \tag{6}$$

$$P_w^t = P_{w2g}^{t} + P_{w2b}^{t} \tag{7}$$

Due to the uncertainties of the outdoor environment, the real wind power generation at the time t can be presented as:

$$P_w^{'} = P_w^t \left(1 + E_w^{t,max} R_t\right) \tag{8}$$

3.1.2. The objective function

The objective function of WPP is to maximize the income denoted by I_w and can be formulated as:

$$max\, I_w = I_{w2g} + I_{w2b} - C_{wm} - C_{wg} \tag{9}$$

3.2. Solar power plant

3.2.1. The trading model

SPP sells electricity to PG at the feed-in tariff and to the buildings at the negotiated prices. Thus, its income can be formulated as follows [12]:

$$I_{s2g} = \sum_{t=1}^{T} p_{s2g} P_{s2g}^{t} \tag{10}$$

$$I_{s2b} = \sum_{t=1}^{T} p_{s2b}^{t} P_{s2b}^{t} \tag{11}$$

The costs of SPP include the maintenance cost C_{sm} and the wheeling cost C_{sg}, which can be formulated as

$$C_{sm} = \sum_{t=1}^{T} \kappa_s P_s^t \tag{12}$$

$$C_{sg} = \sum_{t=1}^{T} \left(\alpha_s {P_{s2b}^{t}}^2 + \beta_s P_{s2b}^{t} \right) \tag{13}$$

The trading electricity amount should satisfy the following:

$$0 \le P_{s2g}^{t} \le P_s^t \tag{14}$$

$$0 \le P_{s2b}^{t} \le P_s^t \tag{15}$$

$$P_s^t = P_{s2g}^{t} + P_{s2b}^{t} \tag{16}$$

Due to the uncertainties of the outdoor environment, the real solar power generation at the time t can be presented as:

$$P_s^{'} = P_s^t \left(1 + E_s^{t,max} R_t\right) \tag{17}$$

3.2.2. The objective function

The objective function of SPP is to maximize the income denoted by I_s and can be formulated as the following:

$$max\, I_s = I_{s2g} + I_{s2b} - C_{sm} - C_{sg} \tag{18}$$

3.3. Buildings

The modeling of the building agent mainly focuses on the thermal dynamic model (TDM) considering the thermal inertia of the building envelope and the trading model.

3.3.1. The TDM of buildings considering envelopes

The TDM of buildings considering envelopes for a single cooling zone is shown in Fig. 2., where a building structure is formulated to describe the dynamic status of the energy transfer and storage [9].

The nodes of TDM are divided into the wall node and the inside room node. Each cooling zone of the buildings has a similar structure and applies the same control method of the AC system to keep the temperature within the comfort range.

By analogy with Newton's law of cooling and Ohm's law, the equation constraints of the wall node and the inside room node are constructed as follows [9]:

$$C_{wall,ij}\left(T_{wall,ij}^{t+1} - T_{wall,ij}^{t}\right) = \Delta t \left(\sum_{j \in N_{wall,n}} \frac{T_j^t - T_{wall,ij}^{t}}{R_{wall,ij}} + r_{ij} v_{ij} A_{wall,ij} Q_{rad,ij} \right) \tag{19}$$

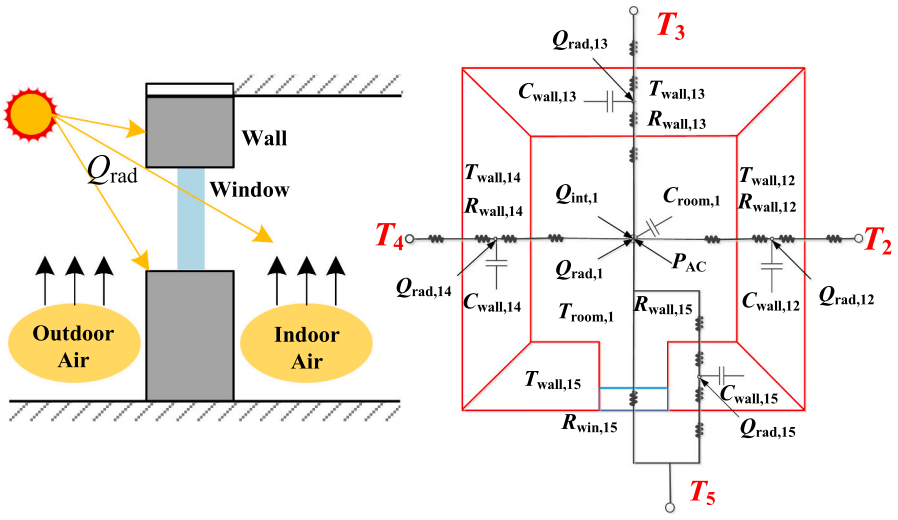

Fig. 2. The diagram of a single cooling zone.

$$C_{\text{room},n}\left(T^{t+1}_{\text{room},n}-T^{t}_{\text{room},n}\right)=\Delta t\left(\sum_{j\in N_{\text{room},n}}\frac{T^{t}_{\text{wall},ij}-T^{t}_{\text{room},n}}{R_{\text{wall},ij}}+\pi_{ij}\sum_{j\in N_{\text{win},n}}\frac{T^{t}_{j}-T^{t}_{\text{room},n}}{R_{\text{win},ij}}\right.$$
$$\left.+E_{\text{EER}}P^{t}_{\text{AC},n}+\pi_{ij}w_{ij}A_{\text{win},ij}Q^{t}_{\text{rad},n}+Q^{t}_{int,n}\right) \tag{20}$$

Due to the uncertainties of the outdoor environment, the real outdoor temperature denoted by $T^{t'}_{\text{out}}$ can be represented as:

$$T^{t'}_{\text{out}}=T^{t}_{\text{out}}\left(1+E^{t,max}_{\text{out}}R_t\right) \tag{21}$$

The indoor temperature should be constrained in a range to guarantee the comfort level of consumers:

$$T^{\min}_{\text{room}}\le T^{t}_{\text{room}}\le T^{\max}_{\text{room}} \tag{22}$$

3.3.2. The trading model of buildings

To guarantee the electricity supply of loads including ACs and save the electricity cost, the buildings would purchase the electricity from PG, WPP, and SPP. Thus, the overall cost of buildings C_{b} can be formulated as follows:

$$C_{\text{b}}=-\left(C_{\text{bg}}+C_{\text{bm}}+I_{\text{w2b}}+I_{\text{s2b}}\right) \tag{23}$$

$$C_{\text{bg}}=\sum\nolimits_{t=1}^{T}p^{t}_{\text{bg}}P^{t}_{\text{bg}} \tag{24}$$

$$C_{\text{bm}}=\sum\nolimits_{t=1}^{T}\left(\kappa_{\text{nm}}P^{t}_{\text{nm}}+\kappa_{\text{AC}}P^{t}_{\text{AC}}\right) \tag{25}$$

$$P^{t}_{\text{bg}}+P^{t}_{\text{w2b}}+P^{t}_{\text{s2b}}=P^{t}_{\text{nm}}+P^{t}_{\text{AC}} \tag{26}$$

$$P^{t}_{\text{AC}}=\Delta t\sum\nolimits_{n\in N_{\text{room}}}P^{t}_{\text{AC},n} \tag{27}$$

The power of ACs should satisfy the range of the following:

$$0\le P^{t}_{\text{AC},n}\le P^{\max}_{\text{AC}} \tag{28}$$

3.3.3. The objective function

The objective function of the buildings is to minimize the overall cost C_{b} and can be formulated as the following:

$$max\ C_{\text{b}}=-\left(C_{\text{bg}}+C_{\text{bm}}+I_{\text{w2b}}+I_{\text{s2b}}\right) \tag{29}$$

4. Solution methodology

4.1. Chance-constrained programming

4.1.1. Reformulation of chance constraints

Because of the thermal inertia, even if the indoor temperature violates the comfortable range, human beings can still tolerate it for some time [38], so the comfort temperature constraint (22) could be relaxed for higher operation flexibility. For this aim, the CCP method can be used to achieve a moderate compromise between optimal objective functions and hard constraints to maintain a certain degree of optimization flexibility [9]. Thus, the indoor temperature can be reformulated as a chance constraint form:

$$Pr\left\{T^{\min}_{\text{room}}\le T^{t}_{\text{room},n}\le T^{\max}_{\text{room}}\right\}\ge\eta \tag{30}$$

4.1.2. Conversion of deterministic constraints

To integrate the chance constraint (30) into the optimization problem, it can be further transformed into a deterministic one.

Assuming that $T^{min,lim}_{\text{room}}$ and $T^{max,lim}_{\text{room}}$ are the limited minimum and maximum indoor temperatures, (30) can be transformed as follows [9]:

$$\begin{cases}T^{\min}_{\text{room}}-\left(1-\gamma^{t}_{n}\right)\left(T^{\min}_{\text{room}}-T^{min,lim}_{\text{room}}\right)\le T^{t}_{\text{room,n}}\\ T^{\max}_{\text{room}}+\left(1-\gamma^{t}_{n}\right)\left(T^{max,lim}_{\text{room}}-T^{\max}_{\text{room}}\right)\ge T^{t}_{\text{room,n}}\end{cases} \tag{31}$$

$$\sum_{n=1}^{N_{\text{room}}}\sum_{t=1}^{T}\gamma^{t}_{n}\ge N_{\text{room}}\cdot T\cdot\eta \tag{32}$$

In the case of $\gamma^{t}_{n}=1$, (31) is the same as (22), which means T^{t}_{room} is completely in the comfort range. In the case of $\gamma^{t}_{n}=0$, (31) becomes

$$T^{min,lim}_{\text{room}}\le T^{t}_{\text{room},n}\le T^{max,lim}_{\text{room}} \tag{33}$$

which means that the indoor temperature is possible to exceed the comfort range but still be limited within $T^{min,lim}_{\text{room}}$ and $T^{max,lim}_{\text{room}}$.

4.2. Nash bargaining

4.2.1. Nash bargaining model

Nash bargaining theory is a type of cooperative game and it can simultaneously take individual and collective interests into account. In this study, Nash bargaining is used for determining the trading electricity amount P^{t}_{w2b} and P^{t}_{s2b}, and the trading prices p^{t}_{w2b} and p^{t}_{s2b}.

The Nash bargaining model designed for our multi-agent energy

system can be formulated as the following [39]:

$$max\ \left(I_w - I_w^0\right)\left(I_s - I_s^0\right)\left(C_b - C_b^0\right) \tag{34}$$

where I_w^0, I_s^0, and C_b^0 are negotiation rupture points for bargaining of WPP, SPP, and the buildings. In the case of non-cooperation, the profits of WPP and SPP consist of the maintenance costs and the income made by selling electricity to PG. Therefore, I_w^0 and I_s^0 can be obtained in the case that WPP and SPP sell all generated electricity to PG with the operation constraints satisfied. C_b^0 can be obtained in the case that the buildings purchase electricity only from PG with the operation constraints and consumers' comfort satisfied.

I_w^0, I_s^0, and C_b^0 should satisfy follows:

$$I_w \geq I_w^0 \tag{35}$$

$$I_s \geq I_s^0 \tag{36}$$

$$C_b \geq C_b^0 \tag{37}$$

4.2.2. Equivalent conversion of Nash bargaining model

The Nash bargaining model in (34) is a nonconvex and nonlinear optimization problem which makes it hard to obtain effective solutions with current algorithms. To facilitate a satisfactory solution, an equivalent conversion is performed to transfer the original problem into two subproblems.

According to the arithmetic mean-geometric mean (AM-GM), inequality (34) meets the following:

$$\left(I_w - I_w^0\right)\left(I_s - I_s^0\right)\left(C_b - C_b^0\right) \leq \left(\frac{I_w + I_s + C_b - I_w^0 - I_s^0 - C_b^0}{3}\right)^3 \tag{38}$$

with equality if and only if

$$\left(I_w - I_w^0\right) = \left(I_s - I_s^0\right) = \left(C_b - C_b^0\right) \tag{39}$$

Therefore, to solve (34), one way is to find the solution of the following first:

$$maxI_w + I_s + C_b - I_w^0 - I_s^0 - C_b^0 \tag{40}$$

Since I_w^0, I_s^0, and C_b^0 are constants, (40) is equivalent to the following:

$$maxI_w + I_s + C_b \tag{41}$$

which can be rewritten as the coalition income subproblem (CIS) as the following:

$$max\ \left(I_{w2g} - C_{wm} - C_{wg}\right) + \left(I_{s2g} - C_{sm} - C_{sg}\right) - \left(C_{bg} + C_{bm}\right) \tag{42}$$

s.t. (1)–(8), (10)–(17), (19)–(28), (30)–(33).

In this subproblem, the multi-agent energy system is treated as a coalition and the objective is to improve the coalition's income. Note that (42) does not contain the transaction values I_{w2b} and I_{s2b} since they are offset. By solving (42), the optimal trading electricity amount $\overline{P}_{w2b}^t$ and $\overline{P}_{s2b}^t$ can be obtained so that the optimal $\overline{I}_{w2g}$, $\overline{C}_{wm}$, $\overline{C}_{wg}$, $\overline{I}_{s2g}$, $\overline{C}_{sm}$, $\overline{C}_{sg}$, $\overline{C}_{bg}$, and $\overline{C}_{bm}$ can be derived as well.

Then Nash bargaining model (34) can be converted into the power payment subproblem (PPS) as follows:

$$\begin{aligned} max\ &\left(I_{w2b} + \overline{I}_{w2g} - \overline{C}_{wg} - \overline{C}_{wm} - I_w^0\right)\left(I_{s2b} + \overline{I}_{s2g} - \overline{C}_{sg} - \overline{C}_{sm} - I_s^0\right) \\ &\left[-\left(I_{w2b} + I_{s2b} + \overline{C}_{bg} + \overline{C}_{bm}\right) - C_b^0\right] \end{aligned} \tag{43}$$

The constraints of (43) include (2), (11), and follows:

$$I_{w2b} + \overline{I}_{w2g} - \overline{C}_{wg} - \overline{C}_{wm} > I_w^0 \tag{44}$$

$$I_{s2b} + \overline{I}_{s2g} - \overline{C}_{sg} - \overline{C}_{sm} > I_s^0 \tag{45}$$

$$-I_{w2b} - I_{s2b} - \overline{C}_{bg} - \overline{C}_{bm} > C_b^0 \tag{46}$$

By solving (43), the optimal trading electricity prices $\overline{p}_{w2b}^t$ and $\overline{p}_{s2b}^t$ can be obtained so that the optimal $\overline{I}_{w2b}$, $\overline{I}_{s2b}$, $\overline{I}_w$, $\overline{I}_s$ and $\overline{C}_b$ are obtained as well.

4.3. Adaptive ADMM

To preserve the privacy of agents, the distributed solution method based on adaptive ADMM with a self-adaptive penalty parameter is applied. In this distributed manner, each agent only needs to share intermediate parameters to obtain the optimal solution.

4.3.1. Distributed models of CIS

The CIS shown in (42) can be converted into

$$\begin{aligned} max\ &\sum_{t=1}^{T}\Big[p_{w2g}P_{w2g}^t + p_{s2g}P_{s2g}^t - p_{bg}^t P_{bg}^t - \left(\alpha_w {P_{w2b}^t}^2 + \beta_w P_{w2b}^t\right) \\ &-\left(\alpha_s {P_{s2b}^t}^2 + \beta_s P_{s2b}^t\right) - \kappa_w P_w^t - \kappa_s P_s^t - \left(\kappa_{nm}P_{nm}^t + \kappa_{AC}P_{AC}^t\right)\Big] \end{aligned} \tag{47}$$

s.t. (1)–(8), (10)–(17), (19)–(28), (30)–(33).

To find the solution to (47), we can transform it from the maximum problem to the minimum problem and apply the ADMM method to protect the privacy of each agent. Define new variables $\widehat{P}_{w2b}^t$ and $\widehat{P}_{s2b}^t$ to denote the electricity amount that the buildings expect to purchase from WPP and SPP, while P_{w2b}^t and P_{s2b}^t denote the electricity amount that WPP and SPP expect to sell to the buildings. It is considered that when $\widehat{P}_{w2b}^t = P_{w2b}^t$ and $\widehat{P}_{s2b}^t = P_{s2b}^t$, the agreement on the trading electricity amount is achieved. Then, with Lagrange multipliers and penalty parameters, (47) can be specialized as:

4.3.1.1. WPP.

The objective function is

$$\begin{aligned} min\ &\Big[\sum_{t=1}^{T}\left(-p_{w2g}P_{w2g}^t + \alpha_w {P_{w2b}^t}^2 + \beta_w P_{w2b}^t + \kappa_w P_{w2b}^t\right) \\ &+\sum_{t=1}^{T}\lambda_w^t\left(\widehat{P}_{w2b}^t - P_{w2b}^t\right) + \frac{\rho_w}{2}\left\|\widehat{P}_{w2b}^t - P_{w2b}^t\right\|_2^2\Big] \end{aligned} \tag{48}$$

s.t. (1)–(8).

4.3.1.2. SPP.

The objective function is

$$\begin{aligned} min\ &\Big[\sum_{t=1}^{T}\left(-p_{s2g}P_{s2g}^t + \alpha_s {P_{s2b}^t}^2 + \beta_s P_{s2b}^t + \kappa_s P_s^t\right) \\ &+\sum_{t=1}^{T}\lambda_s^t\left(\widehat{P}_{s2b}^t - P_{s2b}^t\right) + \frac{\rho_s}{2}\left\|\widehat{P}_{s2b}^t - P_{s2b}^t\right\|_2^2\Big] \end{aligned} \tag{49}$$

s.t. (10)–(17).

4.3.1.3. Buildings.

The objective function is

$$\begin{aligned} min\ &\Big[\sum_{t=1}^{T}\left(p_{bg}^t P_{bg}^t + \kappa_{nm}P_{nm}^t + \kappa_{AC}P_{AC}^t\right) \\ &+\sum_{t=1}^{T}\lambda_w^t\left(\widehat{P}_{w2b}^t - P_{w2b}^t\right) + \sum_{t=1}^{T}\lambda_s^t\left(\widehat{P}_{s2b}^t - P_{s2b}^t\right) \\ &+\frac{\rho_w}{2}\left\|\widehat{P}_{w2b}^t - P_{w2b}^t\right\|_2^2 + \frac{\rho_s}{2}\left\|\widehat{P}_{s2b}^t - P_{s2b}^t\right\|_2^2\Big] \end{aligned} \tag{50}$$

s.t. (19)–(28), (30)–(33).

4.3.2. Distributed models of PPS

The PPS shown in (43) can be converted into

$$max\left[\left(\sum_{t=1}^{T}p_{w2b}^{t}\overline{P}_{w2b}^{t}+\overline{I}_{w2g}-\overline{C}_{wg}-\overline{C}_{wm}-I_{w}^{0}\right)\left(\sum_{t=1}^{T}p_{s2b}^{t}\overline{P}_{s2b}^{t}+\overline{I}_{s2g}-\overline{C}_{sg}-\overline{C}_{sm}-I_{s}^{0}\right)\left(-\sum_{t=1}^{T}p_{w2b}^{t}\overline{P}_{w2b}^{t}-\sum_{t=1}^{T}p_{s2b}^{t}\overline{P}_{s2b}^{t}-\overline{C}_{bg}-\overline{C}_{bm}-C_{b}^{0}\right)\right] \tag{51}$$

s.t. (2), (11), (44)–(46).

To protect the benefits of WPP and SPP intuitively, assume that WPP and SPP trade with buildings at higher prices than those with PG, i.e.,

$$p_{w2g}<p_{w2b}^{t},\widehat{p}_{w2b}^{t} \tag{52}$$

$$p_{s2g}<p_{s2b}^{t},\widehat{p}_{s2b}^{t} \tag{53}$$

To find the solution to (51), we can take the logarithm, transform it from the maximum problem to the minimum problem, and apply the ADMM method to protect the privacy of each agent. Define $\widehat{p}_{w2b}^{t}$ and $\widehat{p}_{s2b}^{t}$ as the trading prices that the buildings expect to pay to WPP and SPP, while p_{w2b}^{t} and p_{s2b}^{t} denote the trading prices that WPP and SPP expect to charge from the buildings. It is considered that when $\widehat{p}_{w2b}^{t}=p_{w2b}^{t}$ and $\widehat{p}_{s2b}^{t}=p_{s2b}^{t}$, the agreement on the trading prices is achieved. Then, with Lagrange multipliers and penalty parameters, (51) can be specialized as follows:

4.3.2.1. WPP. The objective function is

$$min\left[-ln\left(\sum_{t=1}^{T}p_{w2b}^{t}\overline{P}_{w2b}^{t}+\overline{I}_{w2g}-\overline{C}_{wm}-\overline{C}_{wg}-I_{w}^{0}\right)+\sum_{t=1}^{T}\gamma_{w}^{t}\left(\widehat{p}_{w2b}^{t}-p_{w2b}^{t}\right)+\frac{\psi_{w}}{2}\sum_{t=1}^{T}\left\|\widehat{p}_{w2b}^{t}-p_{w2b}^{t}\right\|_{2}^{2}\right] \tag{54}$$

s.t. (2), (44), (52).

4.3.2.2. SPP. The objective function is

$$min\left[-ln\left(\sum_{t=1}^{T}p_{s2b}^{t}\overline{P}_{s2b}^{t}+\overline{I}_{s2g}-\overline{C}_{sm}-\overline{C}_{sg}-I_{s}^{0}\right)+\sum_{t=1}^{T}\gamma_{s}^{t}\left(\widehat{p}_{s2b}^{t}-p_{s2b}^{t}\right)+\frac{\psi_{s}}{2}\sum_{t=1}^{T}\left\|\widehat{p}_{s2b}^{t}-p_{s2b}^{t}\right\|_{2}^{2}\right] \tag{55}$$

s.t. (11), (45), (53).

4.3.2.3. Buildings. The objective function is

$$min\left[-ln\left(-\sum_{t=1}^{T}p_{w2b}^{t}\overline{P}_{w2b}^{t}-\sum_{t=1}^{T}p_{s2b}^{t}\overline{P}_{s2b}^{t}-\overline{C}_{bg}-\overline{C}_{bm}-C_{b}^{0}\right)+\sum_{t=1}^{T}\gamma_{w}^{t}\left(\widehat{p}_{w2b}^{t}-p_{w2b}^{t}\right)+\sum_{t=1}^{T}\gamma_{s}^{t}\left(\widehat{p}_{s2b}^{t}-P_{s2b}^{t}\right)+\frac{\psi_{w}}{2}\sum_{t=1}^{T}\left\|\widehat{p}_{w2b}^{t}-p_{w2b}^{t}\right\|_{2}^{2}+\frac{\psi_{s}}{2}\sum_{t=1}^{T}\left\|\widehat{p}_{s2b}^{t}-p_{s2b}^{t}\right\|_{2}^{2}\right] \tag{56}$$

s.t. (2), (11), (46), (52), (53).

4.3.3. Distributed solving process

The overall flow chart of the distributed solution based on adaptive ADMM for CIS and PPS is shown in Fig. 3. [17].

Take the CIS as an example to illustrate the solving process. Define

$$\|r_{w}(k+1)\|_{2}^{2}=\sum_{t=1}^{T}\left\|\widehat{P}_{w2b}^{t}(k+1)-P_{w2b}^{t}(k+1)\right\|_{2}^{2} \tag{57}$$

$$\|r_{s}(k+1)\|_{2}^{2}=\sum_{t=1}^{T}\left\|\widehat{P}_{s2b}^{t}(k+1)-P_{s2b}^{t}(k+1)\right\|_{2}^{2} \tag{58}$$

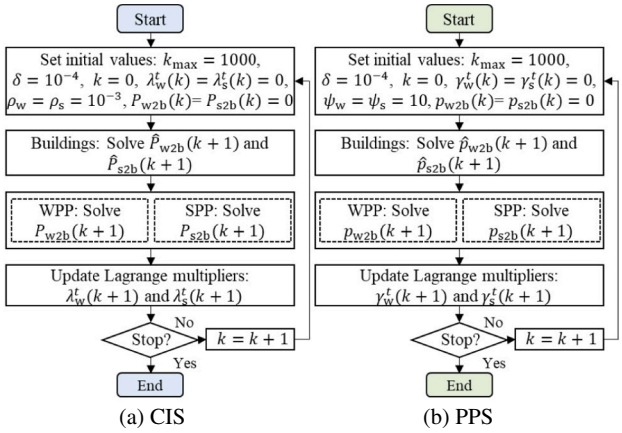

Fig. 3. The flow chart of the distributed solution.

$$\|s_{w}(k+1)\|_{2}^{2}=\sum_{t=1}^{T}\left\|\widehat{P}_{w2b}^{t}(k+1)-\widehat{P}_{w2b}^{t}(k)\right\|_{2}^{2} \tag{59}$$

$$\|s_{s}(k+1)\|_{2}^{2}=\sum_{t=1}^{T}\left\|\widehat{P}_{s2b}^{t}(k+1)-\widehat{P}_{s2b}^{t}(k)\right\|_{2}^{2} \tag{60}$$

The penalty parameters are updated based on the following to achieve rapid convergence:

$$\rho_{w}(k+1)=\begin{cases}\rho_{w2b}(k)\cdot\tau^{incr}, \text{if } \|r_{w}(k+1)\|_{2}\geq\theta\|s_{w}(k+1)\|_{2}\\ \rho_{w2b}(k)/\tau^{decr}, \text{if } \|s_{w}(k+1)\|_{2}\geq\theta\|r_{w}(k+1)\|_{2}\\ \rho_{w2b}(k), \text{otherwise}\end{cases} \tag{61}$$

$$\rho_{s}(k+1)=\begin{cases}\rho_{s2b}(k)\cdot\tau^{incr}, \text{if } \|r_{s}(k+1)\|_{2}\geq\theta\|s_{s}(k+1)\|_{2}\\ \rho_{s2b}(k)/\tau^{decr}, \text{if } \|s_{s}(k+1)\|_{2}\geq\theta\|r_{s}(k+1)\|_{2}\\ \rho_{s2b}(k), \text{otherwise}\end{cases} \tag{62}$$

The Lagrange multipliers are updated as:

$$\lambda_{w}^{t}(k+1)=\lambda_{w}^{t}(k)+\rho_{w}(k+1)\cdot\left(\widehat{P}_{w2b}^{t}(k+1)-P_{w2b}^{t}(k+1)\right) \tag{63}$$

$$\lambda_{s}^{t}(k+1)=\lambda_{s}^{t}(k)+\rho_{s}(k+1)\cdot\left(\widehat{P}_{s2b}^{t}(k+1)-P_{s2b}^{t}(k+1)\right) \tag{64}$$

The stopping condition of iteration is:

$$\begin{cases}max\left(\sum_{t=1}^{T}\left\|\widehat{P}_{w2b}^{t}(k)-P_{w2b}^{t}(k)\right\|_{2}^{2},\sum_{t=1}^{T}\left\|\widehat{P}_{s2b}^{t}(k)-P_{s2b}^{t}(k)\right\|_{2}^{2}\right)<\delta\\ \text{or}\quad k>k_{max}\end{cases} \tag{65}$$

5. Case studies

In this section, the proposed CCP-based distributed cooperative operation strategy for the multi-agent energy system integrated with wind, solar, and buildings is verified. The CIS and PPS are solved by GUROBI and IPOPT, respectively in MATLAB platform on a PC with Intel Core i7 2.30 GHz and 16.0 GB.

5.1. Case setting

The hourly forecasted values of day-ahead market prices which are obtained from the PJM historical market price data, normal loads of buildings, and maximum wind and solar power GCs, are shown in Fig. 4 [9], [12], [40]. The solar radiation and outdoor temperature are shown in Fig. 5 [9].

The maximum power of an AC in a single room is 2 kW and the energy efficiency ratio of ACs is 3.0 [9]. The total operation horizon T is set as 24 h. According to the thermoneutral temperature range of

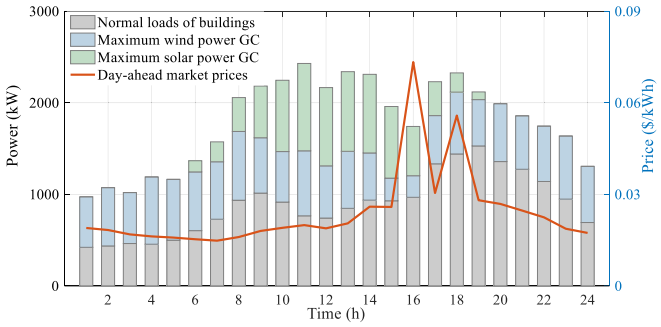

Fig. 4. Forecasted values of day-ahead market prices, normal loads of buildings, and maximum wind and solar GCs.

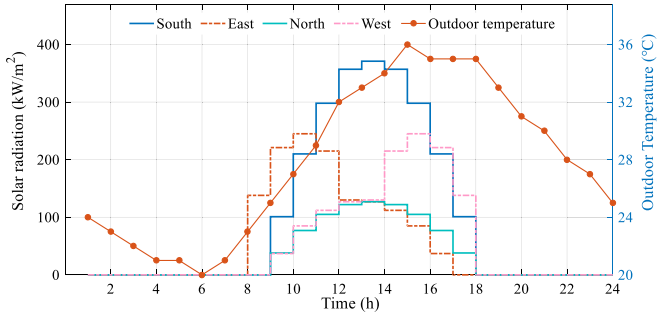

Fig. 5. The solar radiation and outdoor temperature.

17 °C–33 °C [41], the lower and upper limits of the comfortable indoor temperature are set at 20 °C and 23 °C in this study, but the proposed method is not limited to this specific temperature range. The relevant parameters of the buildings are shown in Table 1. Relevant parameters of WPP and SPP are shown in Table 2.

5.2. Results about the iterative process of CIS and PPS

Fig. 6. shows the iterative process of solving CIS which is solved based on the adaptive ADMM method. The agreement on trading electricity amount among WPP, SPP, and the buildings is achieved after 57 iterations. The results are approximately the same as those solved by the centralized method, with 1.21% difference.

Fig. 7. shows the iterative process of solving PPS which is solved based on the adaptive ADMM method. The agreement on trading electricity prices among WPP, SPP, and the buildings is achieved after 347 iterations. The results are approximately the same as those solved by the centralized method, with 0.82% difference.

In the iterative process of solving CIS and PPS, the exchanged information among three agents is only the expected trading electricity amount and trading prices respectively. Based on the exchanged information, WPP, SPP, and the buildings can solve their respective objective functions locally and independently, without transmitting other essential and private information including a great number of related constants and variables. Thus, the privacy of three agents is effectively protected and the amount of information collection and transmission can be reduced by the distributed method based on the adaptive ADMM.

Table 1
Parameters of buildings [9].

Parameter	Value	Parameter	Value
R_{wall}	6×10^{-2} °C/W	$C_{\text{wall(win)}}$	1×10^{7} J/K
$R_{\text{wall(win)}}$	8×10^{-2} °C/W	C_{room}	1×10^{7} J/K
R_{win}	2×10^{-2} °C/W	κ_{nm}	2.2×10^{-3}
C_{wall}	7.9×10^{5} J/K	κ_{AC}	2.2×10^{-3}

Table 2
Parameters of WPP and SPP [12], [42].

Parameter	Value	Parameter	Value
p_{w2g}	0.018$/kWh	p_{s2g}	0.015$/kWh
κ_{w}	8×10^{-4}	κ_{s}	8.5×10^{-4}
α_{w}	3×10^{-7}	α_{s}	3×10^{-7}
β_{w}	5×10^{-4}	β_{s}	5×10^{-4}

5.3. Results about the power of buildings

Fig. 8. shows the power of ACs. The relation between the power of ACs and the indoor temperature is shown in Fig. 8. (a). The indoor temperature is completely constrained in the comfort range of 20 °C to 23 °C. In 9:00–11:00 and 13:00–20:00, the power of ACs is zero or almost zero so the indoor temperature keeps increasing. In 1:00–6:00 and 21:00–24:00, the power of ACs is low as well, but the indoor temperature sustains near the upper limit of 23 °C without violating it. This is because the buildings can store the cooling energy due to the thermal inertia. Otherwise, the indoor temperature may increase more rapidly or violate the upper limit. This result illustrates that the proposed strategy can fully utilize the operation of ACs and the building thermal inertia. Based on this, the energy consumption of ACs is reduced.

Fig. 8. (b) shows the relation between the power of ACs and day-ahead market prices. At 7:00, the electricity price is the lowest and ACs operate at the highest power 2 kW. In 7:00–11:00, the electricity price keeps increasing and in 7:00–8:00, ACs operate at the power which can make the indoor temperature decrease to the lower limit of 20 °C. At 12:00, the electricity price reaches a valley and ACs operate at the relatively high power to make the indoor temperature reach the lower limit again. In 13:00–20:00, especially at 16:00 and 18:00, the electricity price is high compared with that in other time periods and the power of ACs is almost zero. From 21:00 to 24:00, the power of ACs increases because the indoor temperature reaches the upper limit at 21:00. If ACs stop operating, the indoor temperature will break the upper limit. Note that ACs operate at the power that makes the indoor temperature maintain at 23 °C and not decrease, to reduce the energy consumption and the electricity cost.

Based on the above analysis, the conclusion is that the proposed strategy can not only meet the consumer demand for the comfort temperature but also reduce the energy consumption and the electricity cost of the buildings.

5.4. Results about the trading electricity amount with SPP, WPP, and PG

Fig. 9. shows the trading electricity amount between WPP and the buildings. From 14:00–22:00, the buildings prefer to purchase electricity from WPP to minimize the electricity cost due to the relatively high electricity prices. From 15:00 to 19:00, particularly, WPP sells all electricity to the buildings.

Fig. 10. shows the trading electricity amount between SPP and the buildings. From 9:00–19:00, the buildings prefer to purchase electricity from SPP to minimize the electricity cost due to the relatively high electricity prices. From 16:00 to 19:00, particularly, SPP sells all electricity to the buildings.

Fig. 11. shows the trading electricity amount between PG and the buildings. At 7:00 and 12:00, the electricity prices are two valleys and the trading electricity amount is high. From 7:00–11:00, the electricity prices keep increasing and the trading electricity amount keeps decreasing. From 16:00–19:00, the electricity prices are high but the buildings still purchase electricity from PG. This result can be further explained by Fig. 12., which shows the overall optimal operation scheme of the buildings. In this period, the electricity amount purchased from WPP and SPP cannot satisfy the overall power consumption of the buildings, so the buildings still need to purchase electricity from PG even at the high electricity prices.

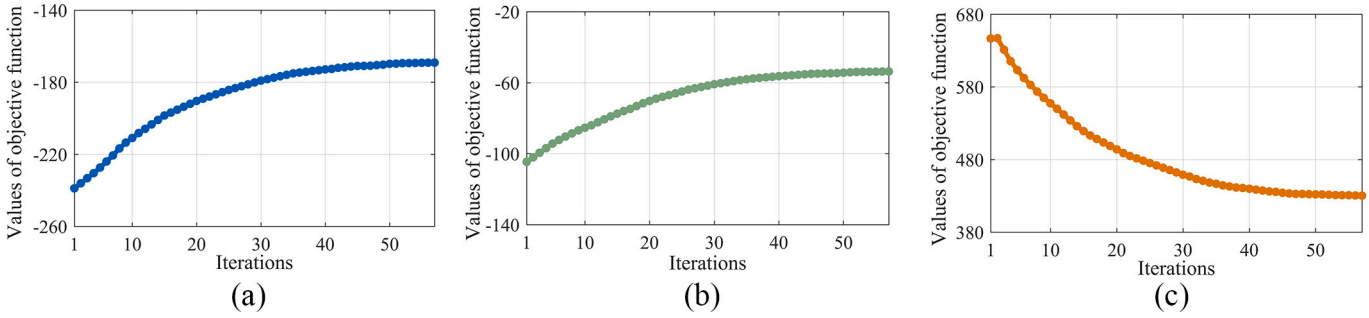

Fig. 6. The iterative process of solving CIS.

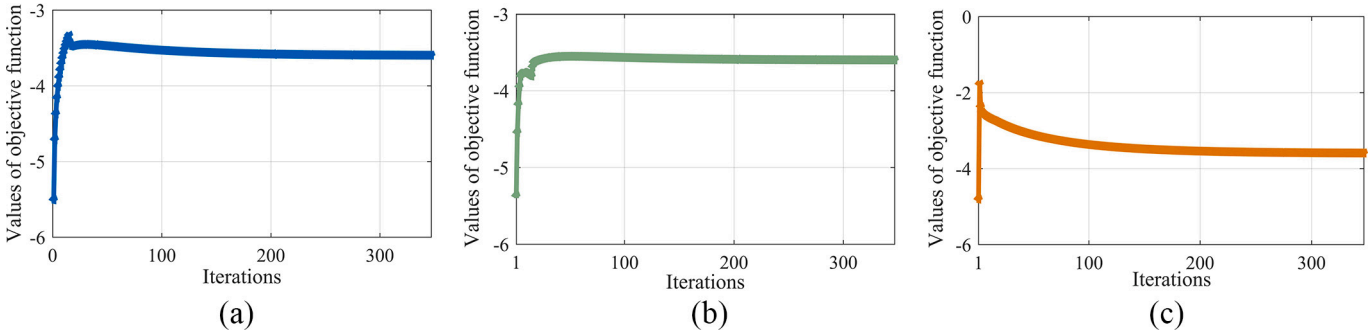

Fig. 7. The iterative process of solving PPS.

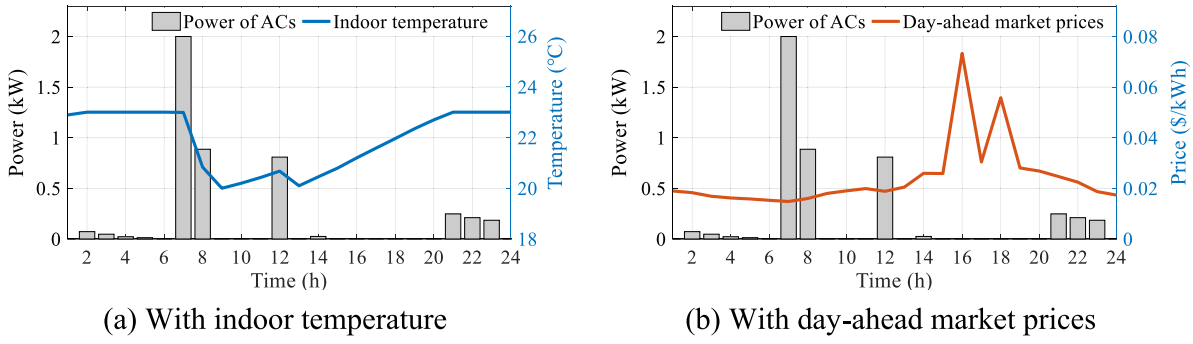

Fig. 8. The power of ACs.

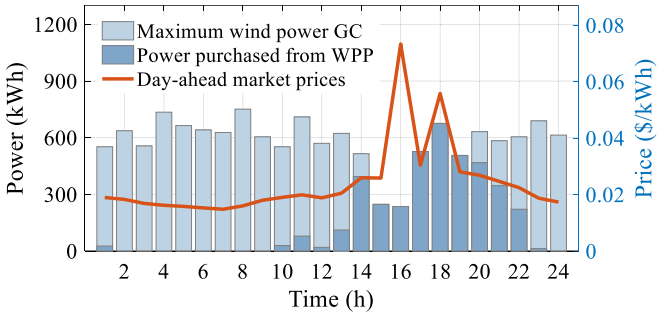

Fig. 9. The power purchased from WPP and day-ahead market prices.

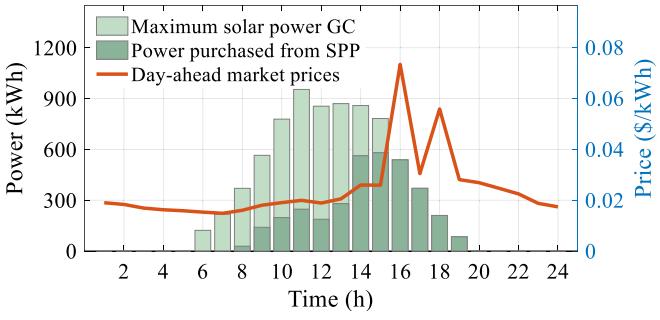

Fig. 10. The power purchased from SPP and day-ahead market prices.

Based on the above analysis, the proposed strategy can promote the consumption of wind and solar power, and it helps the buildings reduce electricity costs since the buildings can purchase electricity from SPP and WPP based on the information on supply, demand, and electricity prices. For PG, the strategy can alleviate the pressure on power supply during peak hours of electricity consumption.

5.5. Results about the prices and the profits

Fig. 13. shows the internal trading prices that the buildings trade

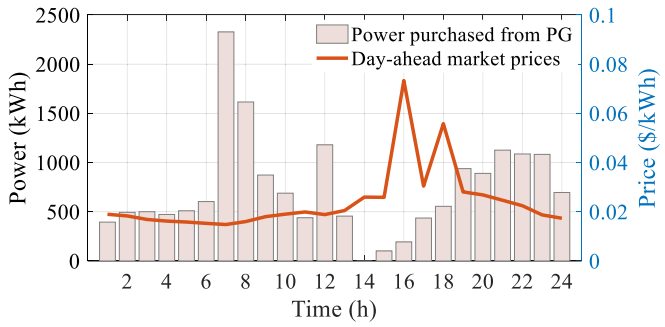

Fig. 11. The power purchased from PG and day-ahead market prices.

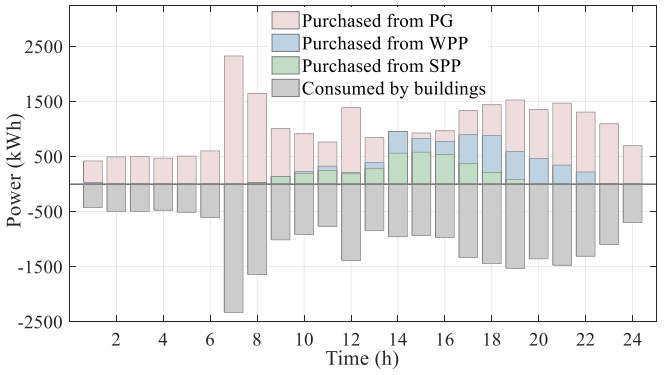

Fig. 12. The overall optimal operation scheme of the buildings.

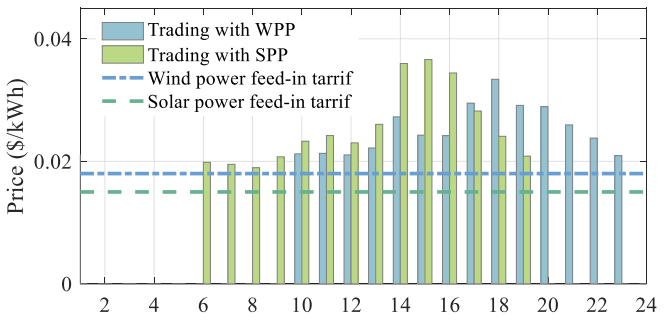

Fig. 13. The prices that the buildings trade with WPP and SPP.

with WPP and SPP. It shows that the trading prices are all higher than the corresponding feed-in tariff. Thus, the price advantage for WPP and SPP based on the proposed strategy is intuitively guaranteed.

It should be noted that the internal trading prices are not unique, since the trading electricity amount has been determined by solving CIS and the transaction value is fixed according to AM-GM inequality shown in (38), which is not directly related to the trading prices. The reason why the distributed method based on the ADMM is proposed is to protect the privacy of each agent.

Table 3 shows the profits when WPP, SPP, and the buildings choose to cooperate based on the proposed strategy or not. Negative values in Table 3 represent costs and positive values represent profits. After cooperation, the overall cost of the coalition decreases from $317.03 to $206.96 and the profits of the three agents increase by $36.69. The results indicate that through cooperation, not only is the overall profit of the coalition improved, but also the profits of each agent increase and are equal, accounting for around one-third of the overall improved profit of the coalition. This shows that the surplus value generated through cooperation is fairly distributed by three agents, demonstrating the fairness of the Nash bargaining method in the distribution of profits since the individual and overall profits are considered simultaneously. Besides, the results are the same as those solved by the method of AM-GM introduced in (38), demonstrating the effectiveness of the distributed solution based on the adaptive ADMM method while the privacy of each agent is protected.

Table 3
Profits of all the agents ($).

Status	WPP	SPP	Buildings	Coalition
Before cooperation	241.73	120.08	−678.84	−317.03
After cooperation	278.42	156.77	−642.15	−206.96
Improved	36.69	36.69	36.69	110.07

5.6. Results and analysis with CCP

In this section, 100 Monte Carlo experiments are carried out to simulate the uncertain environment from wind and solar power generation, and outdoor temperature.

5.6.1. Results about the indoor temperature

To analyze the indoor temperature and the power of ACs, one Monte Carlo experiment at each confidence level is taken as an example.

Fig. 14. shows the indoor temperature of each room in a single building. As the confidence level decreases, the following changes can be observed: the time period that the indoor temperature outside the comfort range becomes longer, with 20:00–23:00 at 90%, 18:00–23:00 at 80%, and 1:00–6:00 and 16:00–24:00 at 70%; the number of rooms where the indoor temperature outside the comfort range becomes greater; the highest indoor temperature becomes higher, with the highest temperature 23 °C at 100%, over 23 °C at 90%, over 24 °C at 80%, and over 25 °C at 70%.

Fig. 15. shows the operating power of ACs in a single building at different confidence levels. In the uncertain outdoor environment, at the 100% confidence level, all ACs operate at the same power, and the temperature is constrained inside the comfort range since the indoor temperature is not allowed to violate the limits. At the 90% confidence level, ACs in different rooms may run at different power since there is the 10% probability that the indoor temperature is outside the comfort range. With confidence levels decreasing, more rooms' ACs will operate at different power, as shown in (c) and (d). Intuitively, the decrease in confidence levels means that the probability that the indoor temperature violates the limits will increase. Therefore, through the flexibility of ACs' operation to adjust the indoor temperature, the buildings, and the multi-agent energy system can operate more flexibly to cope with the impacts of the uncertain environment. It should be noted that due to the low probability and short duration of extreme scenarios, the consumers' comfort will not be significantly influenced.

5.6.2. Results about the profits

Table 4 shows the average profits from the 100 Monte Carlo experiments when the CCP method is applied. It shows that with confidence levels decreasing, the profits of each agent and coalition increase. Essentially, the decrease in confidence levels means that under the uncertain outdoor environment, the buildings may place greater emphasis on the economy by reducing the consumers' comfort. However, the consumers' comfort will not be affected significantly because of the low probability and short duration of extreme scenarios.

Based on the discussion above, the use of the CCP method enables the multi-agent energy system to operate flexibly by adjusting the operating power of ACs to cope with uncertainties from wind and solar power generation, and outdoor temperature. By setting a reasonable confidence level, the strategy based on CCP can take both the economy of the multi-agent energy system and the consumers' comfort into account, and make a moderate compromise according to the real situation and

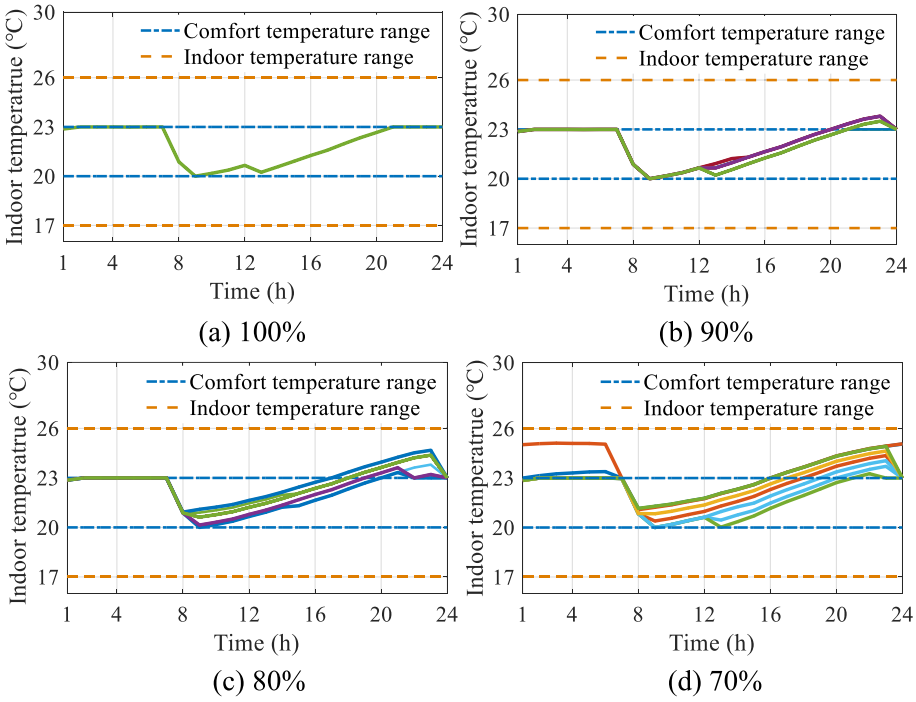

Fig. 14. The comparison of indoor temperature results inside each room at different confidence levels.

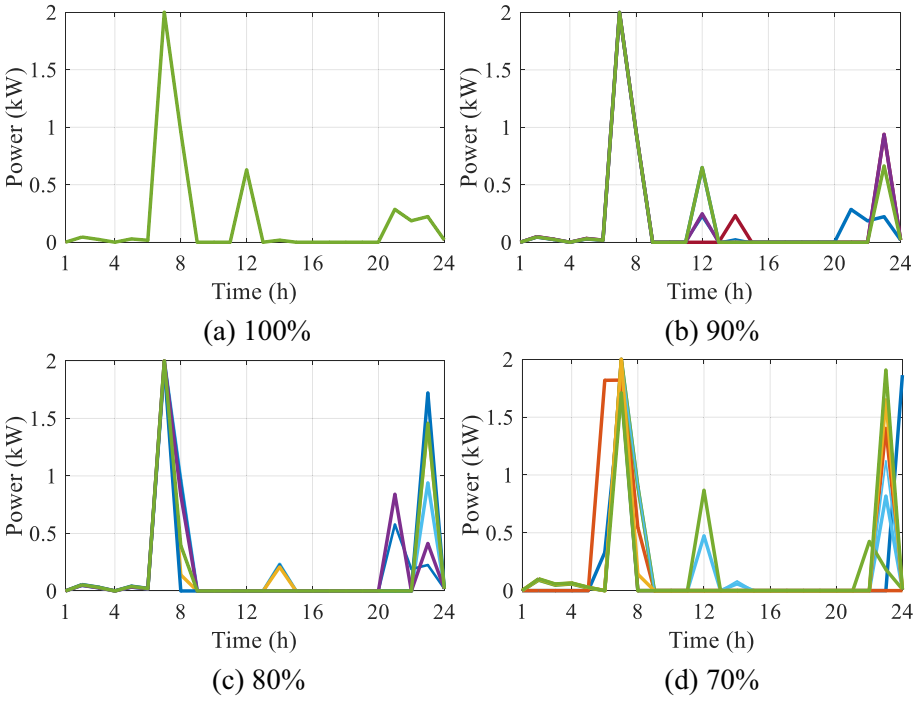

Fig. 15. The comparison of the operating power of ACs at different confidence levels.

requirements.

6. Conclusions

This paper proposes a CCP-based distributed cooperative operation strategy for the multi-agent energy system integrated with wind, solar, and buildings. The following conclusions can be derived:

(1) The proposed market mechanism builds an interactive relationship between WPP and the buildings, as well as SPP and the buildings. Based on the information on electricity demand and prices, the buildings can purchase electricity from WPP and SPP to reduce costs.

(2) In an uncertain environment from wind and solar power generation, and outdoor temperature, the ACs' operation flexibility based on the building thermal inertia can be fully used to obtain the optimal strategy that considers both the operation economy

Table 4
Profits with CCP ($).

Confidence level	WPP	SPP	Buildings	Coalition
100%	278.05	156.40	−642.54	−208.09
Improved	36.32	36.32	36.30	108.94
90%	279.06	157.41	−641.53	−205.06
Improved	37.33	37.33	37.31	111.97
80%	280.49	158.85	−640.10	−200.76
Improved	38.76	38.77	38.74	116.27
70%	281.64	160.00	−638.94	−197.30
Improved	39.91	39.92	39.90	119.73

of the buildings and the consumers' comfort through the CCP method. As confidence levels decrease, the flexible operation of the multi-agent energy system can be further enabled.

(3) Based on the adaptive ADMM method, the subproblems of coalition income and power payment are effectively solved in a distributed way. Through this method, during the trading process, WPP, SPP, and the buildings can solve the objective functions locally and the only information that needs to be exchanged is the expected trading electricity amount and prices. Thus, the issue of privacy protection for engaged agents is effectively solved. At the same time, the efforts made to collect and transmit information can be reduced accordingly.

Our future work will focus on the profit distribution method considering the agents' contributions, to further improve the cooperative operation strategy and motivate agents to participate in the cooperation.

CRediT authorship contribution statement

Bing Ding: Writing – original draft, Software, Conceptualization, Methodology. **Zening Li:** Writing – review & editing, Supervision. **Zhengmao Li:** Writing – review & editing. **Yixun Xue:** Writing – review & editing. **Xinyue Chang:** Writing – review & editing. **Jia Su:** Writing – review & editing. **Xiaolong Jin:** Writing – review & editing. **Hongbin Sun:** Supervision.

Declaration of competing interest

The authors declare that they have no known competing financial interests or personal relationships that could have appeared to influence the work reported in this paper.

Data availability

The data that has been used is confidential.

Acknowledgements

This work was supported by Shanxi Province Natural Science Foundation for Youths (202303021212057) and National Natural Science Foundation of China (U22A6007, 52307131).

References

[1] IEA. World Energy Outlook 2021. Paris: IEA; 2021 [Online]. Available: https://www.iea.org/reports/world-energy-outlook-2021. License: CC BY 4.0.
[2] Bhattarai U, et al. Assay of renewable energy transition: a systematic literature review. Sci Total Environ 2022;833:155159.
[3] Haas C, Kempa K, Moslener U. Dealing with deep uncertainty in the energy transition: what we can learn from the electricity and transportation sectors. Energy Policy 2023;179:113632.
[4] Renewable capacity highlights [Online]. Available: https://www.irena.org/Publications/2023/Mar/-/media/4F25671B76C740A3957F235744AE36A1.ashx; 2024.
[5] Renewable energy industry report [Online]. Available: https://www.ibef.org/industry/renewable-energy; 2024.
[6] Buying clean electricity [Online]. Available: https://www.energy.gov/energysaver/buying-clean-electricity; 2024.
[7] Delmastro C, et al. Buildings. IEA; 2022 [Online]. Available: https://www.iea.org/reports/buildings.
[8] Delmastro C, Martinez-Gordon R. Space cooling. Paris: IEA; Sep. 2022 [Online]. Available: https://www.iea.org/reports/space-cooling.
[9] Su S, Li Z, Jin X, Yamashita K, Xia M, Chen Q. Bi-level energy management and pricing for community energy retailer incorporating smart buildings based on chance-constrained programming. Int J Electr Power Energy Syst 2022;138:107894.
[10] Wang Y, Qiu J, Tao Y, Zhao J. Carbon-oriented operational planning in coupled electricity and emission trading markets. IEEE Trans Power Syst 2020;35(4):3145–57.
[11] The energy conservation (amendment) bill [Online]. Available: https://prsindia.org/billtrack/the-energy-conservation-amendment-bill-2022; 2022.
[12] Ma T, et al. Cooperative operation method for wind-solar-hydrogen multi-agent energy system based on Nash bargaining theory. Proc CSEE 2021;41:25–39.
[13] Wang H, Huang J. Cooperative planning of renewable generations for interconnected microgrids. IEEE Trans Smart Grid 2016;7(5):2486–96.
[14] Guo J, Li Y, Shen Y, Yu J, Chen Y. A novel incentive mechanism for CCHP-based microgrids in spinning reserve. IEEE Trans Power Syst 2021;36(3):1697–712.
[15] Lu Z, Wang J, Shahidehpour M, Bai L, Xiao Y, Li H. Cooperative operation of distributed energy resources and thermal power plant with a carbon-capture-utilization-and-storage system. IEEE Trans Power Syst 2023:1–15.
[16] Qiu R, Zhang H, Wang G, Liang Y, Yan J. Green hydrogen-based energy storage service via power-to-gas technologies integrated with multi-energy microgrid. Appl Energy 2023;350:121716.
[17] Ding J, Gao C, Song M, Yan X, Chen T. Optimal operation of multi-agent electricity-heat-hydrogen sharing in integrated energy system based on Nash bargaining. Int J Electr Power Energy Syst 2023;148:108930.
[18] Xu Y, et al. A coordinated optimal scheduling model with Nash bargaining for shared energy storage and multi-microgrids based on two-layer ADMM. Sustain Energy Technol 2023;56:102996.
[19] Mei S, Wang Y, Liu F, Zhang X, Sun Z. Game approaches for hybrid power system planning. IEEE Trans Sustain Energy 2012;3(3):506–17.
[20] Zhao T, Choo FH, Zhang L, Gu Y, Wang P. Game theory based distributed energy trading for microgrids parks. In: 2017 Asian conf. energ., power & transp elect (ACEPT); 2017. p. 1–7.
[21] Akgün M, Soykan EU, Soykan G. A privacy-preserving scheme for smart grid using trusted execution environment. IEEE Access 2023;11:9182–96.
[22] Li Z, Su S, Jin X, Xia M, Chen Q, Yamashita K. Stochastic and distributed optimal energy management of active distribution network with integrated office buildings. CSEE J Power Energy Syst 2022:1–12.
[23] Huang Z, Hu R, Guo Y, Chan-Tin E, Gong Y. DP-ADMM: ADMM-based distributed learning with differential privacy. IEEE Trans Inf Foren Secur 2020;15:1002–12.
[24] Wang L, et al. Security constrained decentralized peer-to-peer transactive energy trading in distribution systems. CSEE J Power Energy Syst 2022;8(1):188–97.
[25] Meng Y, Ma G, Yao Y, Li H. Nash bargaining based integrated energy agent optimal operation strategy considering negotiation pricing for tradable green certificate. Appl Energy 2024;356:122427.
[26] Song M, et al. Exergy-driven optimal operation of virtual energy station based on coordinated cooperative and Stackelberg games. Appl Energy 2024;360:122770.
[27] Kou X, Zhang X, Merkli S, Agliati V, Kamgarpour M, Lygeros J. A comprehensive scheduling framework using SP-ADMM for residential demand response with weather and consumer uncertainties. IEEE Trans Power Syst 2021;36(4):3004–16.
[28] Rey F, et al. Strengthening the group: aggregated frequency reserve bidding with ADMM. IEEE Trans Smart Grid 2019;10(4):3860–9.
[29] Wang Y, Qiu J, Tao Y. Robust energy systems scheduling considering uncertainties and demand side emission impacts. Energy 2022;239:122317.
[30] Xie R, et al. BESS frequency regulation strategy on the constraints of planned energy arbitrage using chance-constrained programming. Energy Rep 2022;8:73–80.
[31] Ghayoor F, Ghannadpour SF, Zaboli A. Power network-planning optimization considering average power not supplied reliability index: modified by chance-constrained programming. Comput Ind Eng 2022;164:107900.
[32] Wu G, et al. Chance-constrained energy-reserve co-optimization scheduling of wind-photovoltaic-hydrogen integrated energy systems. Int J Hydrog Energy 2023;48(19):6892–905.
[33] Xia W, Ren Z, Qin H, Dong Z. A coordinated operation method for networked hydrogen-power-transportation system. Energy 2024;296:131026.
[34] Wen Y, Hu Z, Chen X, Bao Z, Liu C. Centralized Distributionally robust chance-constrained dispatch of integrated transmission-distribution systems. IEEE Trans Power Syst 2024;39(2):2947–59.
[35] Sun Y, Bahrami S, Wong VWS, Lampe L. Chance-constrained frequency regulation with energy storage systems in distribution networks. IEEE Trans Smart Grid 2020;11(1):215–28.
[36] Ge X, et al. Blockchain and green certificates based market structure and transaction mechanism of direct power-purchase for industrial users. IEEE Trans Ind Appl 2023;59(3):2892–903.
[37] Yu CW. Long-run marginal cost based pricing of interconnected system wheeling. Electr Power Syst Res 1999;50(3):205–12.
[38] Li Z, Xu Y, Wu L, Zheng X. A risk-averse adaptively stochastic optimization method for multi-energy ship operation under diverse uncertainties. IEEE Trans Power Syst 2021;36(3):2149–61.

[39] Wang Y, Zheng Y, Yang Q. Nash bargaining based collaborative energy management for regional integrated energy systems in uncertain electricity markets. Energy 2023;269:126725.
[40] PJM - markets & operations, data miner2 [Online]. Available: https://dataminer2.pjm.com; 2018.
[41] Nicol JF, Humphreys M, Roaf S, et al. Standards for thermal comfort: Indoor air temperature standards for the 21st century. London: Taylor and Francis; 1995.
[42] Couture TD, Cory KS. State clean energy policies analysis (SCEPA) project: An analysis of renewable energy feed-in tariffs in the United States (revised). 2009.